



Exploring the frequency and clinical background of the “zebra sign” in amyotrophic lateral sclerosis and multiple system atrophy



Atsuhiko Sugiyama^{a,b}, Noriko Sato^{c,*}, Yukio Kimura^c, Yoko Shigemoto^{b,c}, Fumio Suzuki^c, Emiko Morimoto^c, Yuji Takahashi^d, Hiroshi Matsuda^b, Satoshi Kuwabara^a

^a Department of Neurology, Graduate School of Medicine, Chiba University, Chiba, Japan

^b Integrative Brain Imaging Center, National Center of Neurology and Psychiatry, Tokyo, Japan

^c Department of Radiology, National Center of Neurology and Psychiatry, Tokyo, Japan

^d Department of Neurology, National Center of Neurology and Psychiatry, Tokyo, Japan

ARTICLE INFO

Keywords:

ALS
MSA
PADRE
Iron
Myelin
Upper motor neuron

ABSTRACT

In amyotrophic lateral sclerosis (ALS), the “zebra sign” in the precentral gyrus on phase difference enhanced magnetic resonance imaging (PADRE) recently has been reported as a possible imaging biomarker for upper motor neuron (UMN) involvement. A previous study has shown that the “zebra sign” allowed us to differentiate patients with ALS from healthy subjects with excellent accuracy. We validated the usefulness of the sign for differentiating patients with ALS from healthy subjects and investigated whether the “zebra sign” can be observed other neurodegenerative disorders with UMN involvement. The “zebra sign” on PADRE was assessed in 26 patients with ALS, 26 with multiple system atrophy (MSA) and 26 healthy controls, and the sign was observed in 50%, 23%, and no subjects, respectively. ALS patients with the “zebra sign” demonstrated a higher UMN burden score than those without the sign. The “zebra sign” on PADRE is not specific to ALS, also present in MSA, but might reflect the degeneration of the UMN within the motor cortex in neurodegenerative disorders.

1. Introduction

Amyotrophic lateral sclerosis (ALS) is a fatal neurodegenerative disorder characterized by loss of upper and lower motor neurons (UMN and LMN) in the primary motor cortex, brainstem, and spinal cord. There is no diagnostic biomarker for ALS, and diagnosis is based on detection of clinical UMN signs, clinical and electrophysiologic LMN signs, and exclusion of other disorders mimicking ALS [1,2]. Clinical signs of UMN impairment may be discrete or often masked by severe LMN involvement [3,4]. Therefore, a reliable UMN biomarker is warranted for early diagnosis, initiation of potential neuroprotective treatments, and recruitment of patients in clinical trials.

A previous study has shown that the “zebra sign” in the precentral gyri in the phase difference enhanced (PADRE) magnetic resonance imaging (MRI) allowed us to differentiate ALS patients from healthy subjects with excellent accuracy and that this sign might reflect degeneration of the UMN in the motor cortex [5]. However, that study included a small number of ALS patients ($n = 16$) and it is unknown whether the “zebra sign” is specific to ALS.

Multiple system atrophy (MSA) is a progressive neurodegenerative disease histologically characterized by the widespread presence of α -

synuclein positive glial cytoplasmic inclusions (GCIs). Pyramidal signs are key clinical features of MSA as well as parkinsonism, cerebellar ataxia, and autonomic failure [6]. A large European MSA cohort study showed that MSA patients frequently have generalized hyperreflexia (43%) and an abnormal plantar reflex (28%) [7]. Previous reports also revealed that some MSA cases had pyramidal dysfunction as the initial presentation and were misdiagnosed as primary lateral sclerosis [8,9]. To date, the “zebra sign” has been evaluated only in ALS, not in other neurodegenerative disorders with UMN involvement, such as MSA.

This study aimed to validate the usefulness of the “zebra sign” for differentiating ALS patients from healthy subjects and investigate the relationship between the “zebra sign” and clinical characteristics. Additionally, to clarify whether the “zebra sign” is specific to ALS or is found in other neurodegenerative disorders with UMN involvement, such as MSA, we assessed the “zebra sign” in not only ALS but also in MSA patients.

* Corresponding author at: Department of Radiology, National Center of Neurology and Psychiatry, 4-1-1 Ogawa-Higashi, Kodaira, Tokyo 187-0031, Japan.
E-mail address: snoriko@ncnp.go.jp (N. Sato).

<https://doi.org/10.1016/j.jns.2019.04.032>

Received 7 March 2019; Received in revised form 8 April 2019; Accepted 23 April 2019

Available online 24 April 2019

0022-510X/ © 2019 Elsevier B.V. All rights reserved.

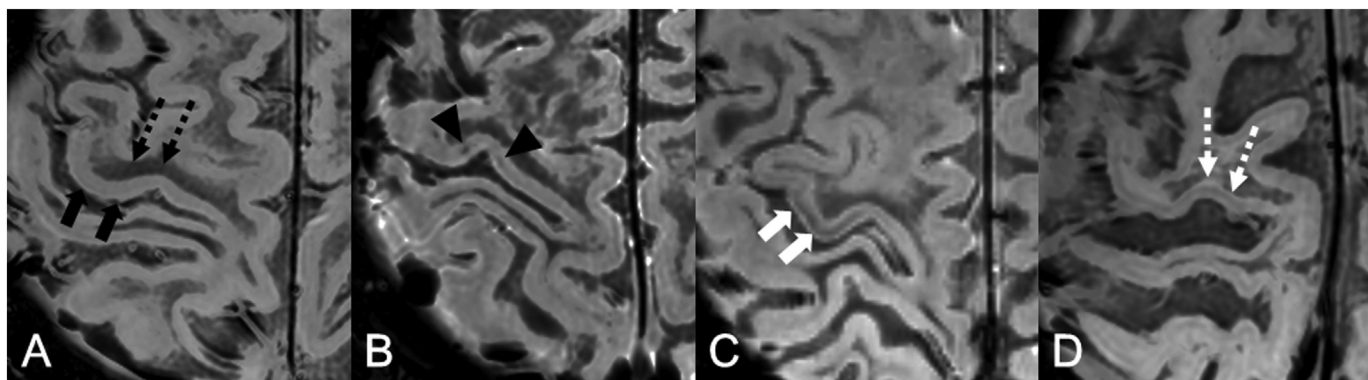


Fig. 1. Negative and positive “zebra signs” in PADRE images

(A) Negative “zebra sign” in a healthy 40-year-old male. The gray matter (*black arrows*) of the precentral gyrus is hyperintense compared to the subcortical white matter (*dotted black arrows*). (B) Negative “zebra sign” in a 61-year-old female MSA patient. A spotty low-signal intensity (*black arrowheads*) is observed in the gray matter of the precentral gyrus. (C) Positive “zebra sign” in a 71-year-old male ALS patient. A LSIL (*white arrows*) is observed in the gray matter of the precentral gyrus. (D) Positive “zebra sign” in a 74-year-old male MSA patient. A LSIL (*white dotted arrows*) is observed in the gray matter of the precentral gyrus.

2. Methods

2.1. Subjects

This retrospective study was approved by the institutional review board at the National Center of Neurology and Psychiatry Hospital, and the need for informed consent was waived.

The following were the inclusion criteria for ALS patients: clinical diagnosis of ALS and 3 Tesla MRI (3 T MRI), including PADRE imaging, between March 2016 and May 2018 at our institution. In all, 32 ALS patients were identified. The following were the exclusion criteria: poor-quality scans for assessment because of artifacts, current or previous history of another central nervous system (CNS) disorder, and abnormal MRI due to another etiology. Of the 32 ALS patients, 4 were excluded because of poor-quality scans due to artifacts and 2 were excluded because of CNS involvement from another etiology (1 with a brain contusion and another with a disproportionately enlarged subarachnoid space hydrocephalus). Finally, 26 ALS patients were included in the study. All were diagnosed according to the Awaji and revised El Escorial criteria (definite 9, probable 12, and possible 5) [1,2].

Additionally, 26 age- and sex-matched MSA patients who underwent 3 T MRI, including PADRE imaging, but did not meet the exclusion criteria described above were enrolled in the study. MSA was diagnosed clinically according to the second consensus statement by Gilman et al. (2008) (probable 18, possible 8) [10].

Furthermore, 26 age- and sex-matched healthy subjects without neurological disorders who volunteered in response to advertisements were used as healthy controls. All of them underwent brain MRI, including PADRE imaging, and did not meet the exclusion criteria described above.

The medical records of the ALS patients were reviewed for age at scan, disease duration, clinical staging, clinical onset, and the Upper Motor Neuron Burden Scale (UMNB). Clinical staging at scan was categorized according to the clinical staging system proposed by Balendra et al. [11]. UMNB measured deep tendon and pathologic reflex scores, producing a scale of 0–45, with higher scores indicating a greater extent of UMN dysfunction [12]. The medical records of the MSA patients were reviewed for age at scan, disease duration, type of disease, and Babinski sign. MSA was classified according to whether the clinical syndrome was dominated by parkinsonism (MSA-P) or cerebellar ataxia (MSA-C).

2.2. MRI studies

All MRI studies were performed on a 3-T MRI system (Philips Medical Systems, Best, The Netherlands). PADRE imaging consisted of

three-dimensional (3D) high-resolution T1 fast-field echo images, which were acquired with parameters of 36 msec/20 msec/6 min 13 s (repetition time/echo time/imaging time), a 23×19.6 cm field of view (FOV), a 320×272 matrix, and 1.0-mm thick sections, which resulted in a voxel size of $0.72 \times 0.72 \times 1.0$ mm³.

The PADRE technique has been described previously [13]. In PADRE imaging, phase differences $\Delta\theta$ are classified and selected, and all are enhanced on the magnitude image $|\rho|$ by the enhancing function $w(\Delta\theta)$. The PADRE image then is reconstructed as:

$$\rho_{\text{PADRE}} = w(\Delta\theta) |\rho|.$$

The reconstitution parameters of PADRE imaging were as follows: low-pass filter size of 48, inverse of a standard deviation of the enhancing function of 4, and phase scaling factor of 1, as used in a previous study [14].

2.3. Image interpretation

Two experienced neuroradiologists blinded to the clinical data independently evaluated the MRI data of each subject. The examiner judged a positive or negative “zebra sign” for each side of the precentral gyrus. In the previous study, appearance of the low-signal intensity layer (LSIL) in the precentral gyri on the PADRE images was divided into the following grades: Grade 0, no low signal intensity area in the precentral gyrus; Grade 1, a spotty low signal intensity area; Grade 2, an LSIL in one or two slices; Grade 3, an LSIL in > 3 slices [5]. The LSIL in the precentral gyrus was defined as a layer with length of > 2 cm parallel to the cortex [5]. When using a cutoff point (Grade 0 and 1 vs. 2 and 3), abnormalities in the precentral gyrus on PADRE imaging for differentiating ALS patients from healthy subjects had a sensitivity, specificity, and accuracy of 94%, 94%, and 94% respectively [5]. According to this previous study, we defined the “zebra sign” as the LSIL in the precentral gyrus with a length of > 2 cm parallel to the cortex (see Fig. 1). A negative “zebra sign” was defined as no or a spotty low signal intensity area in the precentral gyrus (see Fig. 1). For findings where the evaluation of the two examiners was different, the final results were determined by a third examiner blinded to the clinical data. In cases with a positive “zebra sign” in precentral gyri, the examiners jointly investigated the appearance of the LSIL in cortices besides precentral gyri.

2.4. Statistical analysis

SPSS software, ver. 25.0 (SPSS Japan, Tokyo, Japan) was used to perform all statistical analyses. The demographic data of the ALS patients, MSA patients, and the healthy subjects were compared using the

Table 1
Demographic and clinical data of the patients with ALS, MSA, and the HCs.

Group	ALS	MSA	HC	P value for group comparison
Total no.	26	26	26	
Age at MRI (years, mean \pm SD) ^a	62.0 \pm 10.4	59.8 \pm 6.8	62.2 \pm 10.2	0.585
Sex (Male:Female) ^b	14:12	14:12	14:12	1.000
Age at onset (years, mean \pm SD) ^c	59.8 \pm 2.1	55.5 \pm 1.4	NA	0.099
Disease duration (years, median, range) ^d	1.4 (0.2–8.8)	3.4 (1.1–14.7)	NA	0.002

MRI, magnetic resonance imaging; SD, standard deviation; NA, not applicable

^a Univariate 1-way analysis of variance (ANOVA)

^b χ^2 test

^c Student's t-test

^d Mann–Whitney *U* test

χ^2 test for sex and univariate 1-way analysis of variance for age at onset. Demographic variables between two groups were analyzed using Student's *t*-test and the Mann–Whitney *U* test for continuous variables, and χ^2 test and Fisher's exact probability test for categorical variables. $P < .05$ was considered statistically significant. Interrater agreements were tested using Cohen's κ statistics.

3. Results

Table 1 shows the demographics of the subject groups included in the study. Disease duration was significantly longer for MSA than for ALS ($P = .002$). Of the 26 ALS patients, 5 had bulbar onset, 8 had upper limb onset, and 13 had lower limb onset. Additionally, 3 were classified as stage 1, 12 as stage 2, and 11 as stage 3 [11]. Clinical characteristics of the ALS and MSA patients are listed in Supplementary Table 1 and Supplementary Table 2, respectively. The κ values for interrater variability between the two examiners were 0.677.

The “zebra sign” on PADRE was found in 13 of 26 ALS patients (50%; bilaterally in eight, unilaterally in five), six of 26 MSA patients (23%; bilaterally in one, unilaterally in five), and none of 26 healthy controls (0%). The “zebra sign” on PADRE imaging was found in 8 of 16 ALS patients (50%) and 1 of 4 MSA patients (25%), all within 2 years of onset. Among the five ALS patients with a unilateral “zebra” sign, the sign was observed in a side opposite to the clinically disabled side in all but one patient. In ALS patients, we did not observe the LSIL in cortices besides precentral gyri. In 1 MSA patient, we observed the LSIL in premotor cortices, in addition to precentral gyri.

A comparison of ALS and MSA patients with and without the “zebra sign” is shown in Table 2 and Table 3, respectively. The UMN score was significantly higher in the ALS patients with than in those without the “zebra sign” ($P = .015$). Although there were trends for a higher proportion of MSA-P and frequency of Babinski sign in the MSA patients with than in those without the “zebra sign,” there was no statistically significant difference.

4. Discussion

Our results demonstrated that the “zebra sign” on PADRE images was observed in half of ALS patients and one-quarter of MSA patients, and was not present in age-matched normal controls. We found that the “zebra sign” is not a specific finding to ALS but can also be observed in neurodegenerative disorders with UMN involvement, such as MSA. Our results also confirmed a previously reported finding that the “zebra sign” has great specificity to distinguish ALS patients from healthy subjects [5]. ALS patients with the “zebra sign” demonstrated a higher UMN score than those without the “zebra sign,” and this sign might reflect degeneration of the UMN within the motor cortex in ALS patients.

The “zebra sign” on PADRE images might reflect iron deposition and reduced concentration of myelin in the precentral gyrus, which was associated with UMN degeneration in ALS. PADRE is a new, developing

Table 2
Comparison of patients with and without zebra sign in ALS.

Characteristics	Zebra sign (n = 13)	No zebra sign (n = 13)	P value
Age at MRI, y, (mean \pm SD) ^a	64.4 \pm 10.1	59.7 \pm 10.5	0.749
Sex (Male/Female) ^b	9/4	5/8	0.116
Duration of disease, y, median (range) ^c	1.3 (0.3–5.8)	1.8 (0.2–8.8)	0.880
Clinical staging, No. of patients ^c			0.511
Stage 1	2	1	
Stage 2	4	8	
Stage 3	7	4	
Clinical onset, No. of patients ^d			1.000
Bulbar	3	2	
Upper limb	4	4	
Lower limb	6	7	
UMNB score (mean \pm SD) ^a	30.2 \pm 5.7	22.5 \pm 9.0	0.015

MRI, magnetic resonance imaging; SD, standard deviation; UMN, Upper Motor Neuron Burden Scale

^a Student's t-test

^b χ^2 test

^c Mann–Whitney *U* test

^d Fisher's exact probability test

MRI method in which contrast of the target tissue is enhanced by selecting the appropriate phase difference between the target and surrounding tissue. PADRE is designed to enhance phase differences on the magnitude image; therefore, it might be sensitive to iron in the forms of hemosiderin, ferritin, and deoxyhemoglobin as well as susceptibility-weighted imaging (SWI) [15]. A previous histologic study of ALS demonstrated iron accumulation in the middle and deep layers of the precentral gyrus corresponding to the location of hypointensity on 3 T MRI fluid-attenuated inversion recovery images and on 7 T T2*-weighted images [16]. Another study also showed the deposition of ferritin in the precentral gyrus in which hypointensity was observed on SWI [17]. The LSIL in the middle and deep gray matter on PADRE might correspond to the iron deposition. It has been reported repeatedly that the extent of signal changes in the precentral cortex, which reflect iron accumulation, correlated with the extent of UMN impairment [16,18–20]. In line with these previous studies, the ALS patients with the “zebra sign” showed significantly higher UMN score than those without the sign in our study.

The high-signal intensity layer adjacent inside the LSIL in the gray matter of the precentral gyrus might corresponded to the deepest portion of gray matter, which was spared iron deposition, and the sub-cortical white matter with reduced concentration of myelin. In healthy subjects, the perirolandic subcortical white matter was seen as a low-signal intensity area on PADRE images, which seems to reflect high myelin density [21]. Histologic study of ALS patients revealed a loss of myelin in the subcortical white matter of the precentral gyrus [16]. The high-signal intensity layer in the superficial gray matter might

Table 3
Comparison of patients with and without zebra sign in MSA.

Characteristics	Zebra sign (n = 6)	No zebra sign (n = 20)	P value
Age at MRI, y, (mean ± SD) ^a	61.7 ± 8.4	59.3 ± 6.3	0.454
Sex (Male/Female) ^b	4/2	10/10	0.652
Duration of disease, y, median (range) ^c	4.3 (1.2–14.7)	3.4 (1.1–7.8)	0.157
Type of disease (MSA-C/MSA-P) ^b	2/4	16/4	0.051
Babinski sign, No. % ^b	4 (66.7)	4 (20.0)	0.051

MRI, magnetic resonance imaging; SD, standard deviation

^a Student's *t*-test

^b Fisher's exact probability test

^c Mann-Whitney *U* test

correspond to the gray matter spared iron deposition. The previous histopathologic study confirmed that the superficial gray matter was spared iron deposition in ALS patients [16].

The “zebra sign” on PADRE images has high specificity for differentiating ALS patients from healthy subjects (100% [excellent] in our study and 94% [very high specificity] in a previous study [5]). Several recent reports have shown the usefulness of the low-signal intensity in the precentral cortices on SWI in ALS patients as an objective indicator of UMN dysfunction [17,20]. On the other hand, low-signal intensity in the precentral gyrus could be observed in normal subjects [17,22]. In the previous study, the “zebra sign” on PADRE showed higher specificity for differentiating ALS from healthy subjects than the low-signal intensity in the precentral cortices on SWI [5]. The reason for this difference in specificity is believed that the finding on SWI corresponded to iron accumulation, whereas the finding on PADRE reflected not only iron content, but also myelin density. Another possible explanation is that SWI is very sensitive enough to detect iron accumulation in healthy subjects, whereas PADRE images used our and the previous study [5] are moderately sensitive enough to detect pathologic iron accumulation associated with UMN impairment, but insufficient to detect iron accumulation in healthy subjects.

Compared to the previous study [5], our study showed that the “zebra sign” on PADRE had relative low sensitivity for the diagnosis of ALS. The reason for this may be that the MRI scanner and reconstitution parameters used in our study were different from those of the previous report [5]. The PADRE program that we used was commercialized software and not optimized for this study. Tailored reconstitution parameters for evaluating the “zebra sign” might improve the diagnostic performance of the sign. However, it is too cumbersome to use different reconstitution parameters for each disorder, and it is meaningful to evaluate the sign using the commercialized reconstitution parameters considering versatility in general clinical practice.

The “zebra sign” can be observed in some MSA patients, and pathologic background of the sign in MSA patients might similar to that in ALS patients. Papp et al. [23,24] described that the primary motor cortex in patients with MSA contained a large number of GCIs. In addition to the presence of GCIs, loss of small- and medium-sized pyramidal cells and astrogliosis have been reported in the primary motor cortex, especially in the fifth and sixth layers [25–29]. The involvement of Betz cells is presumed to be different for each case [29]. Degeneration of the subcortical white matter adjacent to the primary motor cortex, which is manifested as loss of myelinated fibers and astrogliosis, also has been reported [24,29]. To date, pathologic iron accumulation in the primary motor cortex has not been confirmed in MSA patients. Ferritin deposition was observed in the putamen and dentate nucleus of the cerebellum [30,31]. Increased tissue iron and ferritin were observed in the pons of MSA tissue [32]. Whether dysregulation of brain iron homeostasis acts as a primary cause of neurodegeneration or is a secondary result of cellular death remains to be elucidated in MSA. It has been suggested that dysregulation of brain iron homeostasis is related to the pathophysiology of MSA via oxidative stress and neuroinflammation [33]. In an imaging study, the T2 low-signal intensity,

which can be related to an increase of iron content, was described in the motor cortex of MSA patients [34]. In 1 MSA patient with a long disease course, we observed the LSIL not only in precentral gyri but also in premotor cortices, and we believe that pathological changes like those in precentral gyri are spread in premotor cortices. A previous pathological reported a decrease in the number of neurons and a high density of GCIs in premotor and supplementary motor areas, especially in patients with a long disease course, although these changes were less prominent compared to precentral gyri [29].

In dementia with Lewy bodies (DLB) and Parkinson's disease (PD), referred to as α -synucleinopathies, as with MSA, Lewy bodies are present in cerebral cortices. However, motor cortices are relatively spared in Parkinson's disease [35], and it is rare that they are mainly involved in Lewy body pathology [36,37]. Therefore, we believe that the “zebra sign” will not be observed in DLB and PD patients.

In this study, there were trends for higher frequency of the Babinski sign and proportion of MSA-P in the MSA patients with than in those without the “zebra sign.” In assessing the extent of UMN involvement, UMN score as calculated in ALS patients seems to be more desirable than Babinski sign alone. Unfortunately, detailed results of reflex to calculate the UMN score were not available in some MSA patients. Pathologic studies suggested that the involvement of neurons and oligodendroglial cells in the motor area was associated with the pathologic alterations of the nigrostriatal pathway [29]. In a study using paired transcranial magnetic stimulation to evaluate the motor cortical excitability change, Marchese et al. [38] reported that patients with MSA-P showed reduced intracortical inhibition, whereas patients with MSA-C showed a normal intracortical inhibition. Another study of transcranial magnetic stimulation using the triple stimulation technique showed that the mean triple stimulation technique ratio for MSA-P was significantly reduced in Parkinson's disease patients and controls, whereas ratios for MSA-C were not different [39]. On the other hand, previous reports showed that hyperreflexia was more common in MSA-C than MSA-P [7,40]. To clarify the association of the “zebra sign” and clinical data including UMN signs and disease type, further large-scale studies with detailed evaluation of UMN signs is needed.

Our study has several limitations. First, we did not have pathologic confirmation, and the possibility of a misdiagnosis in some cases cannot be excluded. Second, we could not assess the correlation with UMN impairment since evaluation of the “zebra sign” is qualitative. Third, we selected MSA patients and healthy subjects as control groups. We could not assess the usefulness of the “zebra sign” for differentiating ALS from ALS mimics in clinical practice. Finally, the relationship between the “zebra sign” in the precentral gyrus on PADRE and the histopathologic changes was not confirmed in ALS and MSA. To confirm the pathophysiological background of the “zebra sign” and its clinical usefulness for differentiating ALS from ALS mimics, further studies are required to evaluate the specific histopathological changes of the “zebra sign” and assessing it in not only ALS but also other motor neuron disorders, including ALS mimics.

In conclusion, the “zebra sign” on PADRE images could reflect degeneration of the UMN within the motor cortex in ALS patients, but not

specific to ALS, observed in some MSA patients.

Supplementary data to this article can be found online at <https://doi.org/10.1016/j.jns.2019.04.032>.

Conflict of interest

The authors declare that they have no conflict of interest.

Acknowledgment

The authors would like to thank Dr. Tetsuya Yoneda who provided support for introducing the software for PADRE to our facility.

References

- [1] B.R. Brooks, R.G. Miller, M. Swash, T.L. Munsat, El Escorial rivisted: revised criteria for the diagnosis of amyotrophic lateral sclerosis, *Amyotroph. Lateral Scler.* 1 (2000) 293–299.
- [2] M. de Carvalho, R. Dengler, A. Eisen, et al., Electrodiagnostic criteria for diagnosis of ALS, *Clin. Neurophysiol.* 119 (2008) 497–503.
- [3] S. Zoccolella, E. Beghi, G. Palagano, et al., Predictors of delay in the diagnosis and clinical trial entry of amyotrophic lateral sclerosis patients: a population-based study, *J. Neurol. Sci.* 250 (2006) 45–49.
- [4] A. Al-Chalabi, O. Hardiman, M.C. Kiernan, et al., Amyotrophic lateral sclerosis: moving towards a new classification system, *Lancet Neurol.* 15 (2016) 1182–1194.
- [5] S. Kakeda, T. Yoneda, S. Ide, et al., Zebra sign of precentral gyri in amyotrophic lateral sclerosis: a novel finding using phase difference enhanced (PADRE) imaging-initial results, *Eur. Radiol.* 26 (2016) 4173–4183.
- [6] N.P. Quinn, C.D. Marsden, The motor disorder of multiple system atrophy, *J. Neurol. Neurosurg. Psychiatry* 56 (1993) 1239–1242.
- [7] M. Köllensperger, F. Geser, J.P. Ndayisaba, et al., Presentation, diagnosis, and management of multiple system atrophy in Europe: final analysis of the European multiple system atrophy registry, *Mov. Disord.* 25 (2010) 2604–2612.
- [8] A.J. da Rocha, A.C. Maia Jr., C.J. da Silva, et al., Pyramidal tract degeneration in multiple system atrophy: the relevance of magnetization transfer imaging, *Mov. Disord.* 22 (2007) 238–244.
- [9] T. Muayqil, K.M. Chan, R. Camicioli, et al., Motor cortex and spinal degeneration in multisystem atrophy: a multimodal study, *Can J Neurol Sci* 35 (2008) 658–660.
- [10] S. Gilman, G.K. Wennin, P.A. Low, et al., Second consensus statement on the diagnosis of multiple system atrophy, *Neurology* 71 (2008) 670–676.
- [11] R. Balendra, A. Jones, N. Jivraj, et al., Use of clinical staging in amyotrophic lateral sclerosis for phase 3 clinical trials, *J. Neurol. Neurosurg. Psychiatry* 86 (2015) 45–49.
- [12] M.J. Alshikho, N.R. Zürcher, M.L. Loggia, et al., Glial activation colocalizes with structural abnormalities in amyotrophic lateral sclerosis, *Neurology* 87 (2016) 2554–2561.
- [13] S. Kakeda, Y. Korogi, T. Yoneda, et al., A novel tract imaging technique of the brainstem using phase difference enhanced imaging: normal anatomy and initial experience in multiple system atrophy, *Eur. Radiol.* 21 (2011) 2202–2210.
- [14] A. Sugiyama, N. Sato, Y. Kimura, et al., MR findings in the substantia nigra on phase difference enhanced imaging in neurodegenerative parkinsonism, *Parkinsonism Relat. Disord.* 48 (2018) 10–16.
- [15] S. Kakeda, Y. Korogi, T. Yoneda, et al., Parkinson's disease: diagnostic potential of high-resolution phase difference enhanced MR imaging at 3 T, *Eur. Radiol.* 23 (2013) 1102–1111.
- [16] J.Y. Kwan, S.Y. Jeong, P.V. Gelderen, et al., Iron accumulation in deep cortical layers accounts for MRI signal abnormalities in ALS: correlating 7 tesla MRI and pathology, *PLoS ONE* 7 (2012) e35241.
- [17] Y. Adachi, N. Sato, Y. Saito, et al., Usefulness of SWI for the detection of iron in the motor cortex in amyotrophic lateral sclerosis, *J. Neuroimaging* 25 (2015) 443–451.
- [18] M. Cosottini, G. Donatelli, M. Costagli, et al., High-resolution 7T MR imaging of the motor cortex in amyotrophic lateral sclerosis, *Am. J. Neuroradiol.* 37 (2016) 455–461.
- [19] M. Costagli, G. Donatelli, L. Biagi, et al., Magnetic susceptibility in the deep layers of the primary motor cortex in amyotrophic lateral sclerosis, *NeuroImage* 12 (2016) 965–969.
- [20] H. Endo, K. Sekiguchi, H. Shimada, et al., Low signal intensity in motor cortex on susceptibility-weighted MR imaging is correlated with clinical signs of amyotrophic lateral sclerosis: a pilot study, *J. Neurol.* 265 (2018) 552–561.
- [21] S. Kakeda, T. Yoneda, S. Ide, et al., Signal intensity of superficial white matter on phase difference enhanced imaging as a landmark of the perirolandic cortex, *Acta Radiol.* 57 (2016) 1380–1386.
- [22] S. Kakeda, Y. Korogi, K. Kamada, et al., Signal intensity of the motor cortex on phase-weighted imaging at 3T, *Am. J. Neuroradiol.* 29 (2008) 1171–1175.
- [23] M.I. Papp, J.E. Kahn, P.L. Lantos, Glial cytoplasmic inclusions in the CNS of patients with multiple system atrophy (striatonigral degeneration, olivopontocerebellar atrophy and shy-Drager syndrome), *J. Neurol. Sci.* 94 (1989) 79–100.
- [24] M.I. Papp, P.L. Lantos, The distribution of oligodendroglial inclusions in multiple system atrophy and its relevance to clinical symptomatology, *Brain* 117 (1994) 235–243.
- [25] T. Fujita, M. Doi, T. Ogata, et al., Cerebral cortical pathology of sporadic olivopontocerebellar atrophy, *J. Neurol. Sci.* 116 (1993) 41–46.
- [26] K. Wakabayashi, T. Ikeuchi, A. Ishikawa, et al., Multiple system atrophy with severe involvement of the motor cortical areas and cerebral white matter, *J. Neurol. Sci.* 156 (1998) 114–117.
- [27] M. Konagaya, M. Sakai, Y. Matsuoka, et al., Multiple system atrophy with remarkable frontal lobe atrophy, *Acta Neuropathol.* 97 (1999) 423–428.
- [28] K. Tsuchiya, E. Ozawa, C. Haga, et al., Constant involvement of the Betz cells and pyramidal tract in multiple system atrophy: a clinicopathological study of seven autopsy cases, *Acta Neuropathol.* 99 (2000) 628–636.
- [29] M. Su, Y. Yoshida, Y. Hirata, et al., Primary involvement of the motor area in association with the nigrostriatal pathway in multiple system atrophy: neuropathological and morphometric evaluations, *Acta Neuropathol.* 101 (2001) 57–64.
- [30] E. Matsusue, S. Fujii, Y. Kanasaki, et al., Putaminal lesion in multiple system atrophy: Postmortem MR-pathological correlations, *Neuroradiology* 50 (2008) 559–567.
- [31] E. Matsusue, S. Fujii, Y. Kanasaki, et al., Cerebellar lesions in multiple system atrophy: Postmortem MR imaging-pathologic correlations, *Am. J. Neuroradiol.* 30 (2009) 1725–1730.
- [32] N.P. Visanji, J.F. Collingwood, M.E. Finnegan, et al., Iron deficiency in parkinsonism: region-specific iron dysregulation in Parkinson's disease and multiple system atrophy, *J. Park. Dis.* 3 (2013) 523–537.
- [33] C. Kaindlstorfer, K.A. Jellinger, S. Eschböck, et al., The relevance of iron in the pathogenesis of multiple system atrophy: a viewpoint, *J. Alzheimers Dis.* 61 (2018) 1253–1273.
- [34] H. Miwa, Y. Kajimoto, I. Nakanishi, et al., T2-low signal intensity in the cortex in multiple system atrophy, *J. Neurol. Sci.* 211 (2003) 85–88.
- [35] H. Braak, U. Rüb, C. Schultz, K. Del Tredici, Vulnerability of cortical neurons to Alzheimer's and Parkinson's diseases, *J. Alzheimers Dis.* 9 (2006) 35–44.
- [36] K. Wakabayashi, F. Mori, Y. Oyama, et al., Lewy bodies in Betz cells of the motor cortex in a patient with Parkinson's disease, *Acta Neuropathol.* 105 (2003) 189–192.
- [37] K. Kasanuki, K.A. Josephs, T.J. Ferman, et al., Diffuse Lewy Body Disease Manifesting as Corticobasal Syndrome, vol. 91, (2018), pp. e268–e279.
- [38] R. Marchese, C. Trompetto, A. Buccolieri, et al., Abnormalities of motor cortical excitability are not correlated with clinical features in atypical parkinsonism, *Mov. Disord.* 15 (2000) 1210–1214.
- [39] A. Eusebio, J.P. Azulay, T. Witjas, et al., Assessment of cortico-spinal tract impairment in multiple system atrophy using transcranial magnetic stimulation, *Clin. Neurophysiol.* 118 (2007) 615–623.
- [40] P.A. Low, S.G. Reich, J. Jankovic, et al., Natural history of multiple system atrophy in North America: a prospective cohort study, *Lancet Neurol.* 15 (2015) 710–719.